Analyst

Journal Name

Continuous measurement of enzymatic kinetics in droplet flow for point-of-care monitoring

Sammer-ul Hassan[a], Adrian M. Nightingale[a] and Xize Niu[a,b†]

Droplet microfluidics is ideally suited to continuous biochemical analysis, requiring low sample volumes and offering high temporal resolution. Many biochemical assays are based on enzymatic reactions, the kinetics of which can be obtained by probing droplets at multiple points over time. Here we present a miniaturised multi-detector flow cell to analyse enzyme kinetics in droplets, with an example application of continuous glucose measurement. Reaction rates and Michaelis–Menten kinetics can be quantified for each individual droplet and unknown glucose concentrations can be accurately determined (errors <5 %). Droplets can be probed continuously giving short sample-to-result time (~30 s) measurement. In contrast to previous reports of multipoint droplet measurement (all of which used bulky microscope-based setups) the flow cell presented here has a small footprint and uses low-powered, low-cost components, making it ideally suited for use in field-deployable devices.

INTRODUCTION

By translating bioanalytical testing from the laboratory into the clinic or at home, point-of-care (POC) diagnostics enable timely diagnosis, monitoring and treatment of patients. Fundamental to the development of POC diagnostics has been the use of microfluidics, which offer small sample volumes and can combine multiple sample-processing steps into a single device.[1] Consequently, microfluidic POC devices have been developed and commercialised for numerous procedures, including a range of assays and tests for quantification of small molecules, nucleic acids and cells.[2]

Thus far POC research has almost exclusively focussed on diagnostic devices – machines that can analyse a specimen to give a single standalone reading. Much less attention has been given to POC monitoring – in which the concentration of fast-changing biomarkers (such as metabolites) are continuously measured to give a continuous readout in much the same way that heart-rate is reported in critical care. In addition to an up-to-date measurement, POC monitoring also provides clinicians with information on the trend and rate of biomarker change over a continuous period, such that they can make more informed decisions. Previous studies on real-time online monitoring of glucose levels in traumatic brain injury [3] and diabetes [4] patients have shown that continuous and rapid monitoring of key analytes (in the time-scale of minutes to tens of seconds) could play critical roles in clinical decision-

making.

Currently research into POC monitoring has exclusively utilised electrochemical probes – either inserted under the skin [5] or by inline measurement of microdialysate.[3, 6-7] Using this method several different analytes (including glucose,[3] lactate,[8] pyruvate,[9] glutamate,[10] and potassium[3, 8]) have been accurately monitored in vivo. Recently, Gao and co-workers developed a non-invasive wearable sensor to measure glucose, lactate, potassium and sodium in the perspiration of human subjects.[11] Importantly electrochemical probes can suffer from surface-fouling and signal drift, which lead to measurement errors over time and limited probe lifetimes.[12] Thus there is a need to develop POC monitoring based on robust analytical methods that can go long periods without recalibration. Colorimetry, in which an analyte-specific reagent (typically enzyme-based for biomolecule analysis) reacts with the target analyte to give a quantifiable coloured product, offers a promising alternative. Colorimetry is well-suited for POC testing, having been successfully applied to accurate quantitative analysis in microfluidics [13-15] and with multiple assays already developed for many metabolites and other important biomarkers.[16]

Droplet-based microfluidics, in which reactions are performed in a flow of nano- or picolitre droplets,[17] is ideally suited for implementing biochemical assays. Dispersion or band-broadening effects are obviated and measurement frequencies can be increased, thus enabling the high throughput analysis required for POC monitoring. [18]

Colorimetric assays for quantifying biomolecules are particularly challenging for POC monitoring, however, as the reactions are typically slow, taking up to an hour to go to completion[19-20]. This means the typical method of end-point quantification is unsuitable for POC monitoring. One way

---

[a.] Faculty of Engineering and the Environment, University of Southampton, Southampton, U.K. SO17 1BJ.

[b.] Institute for Life Sciences, University of Southampton, Southampton, U.K. SO17 1BJ.
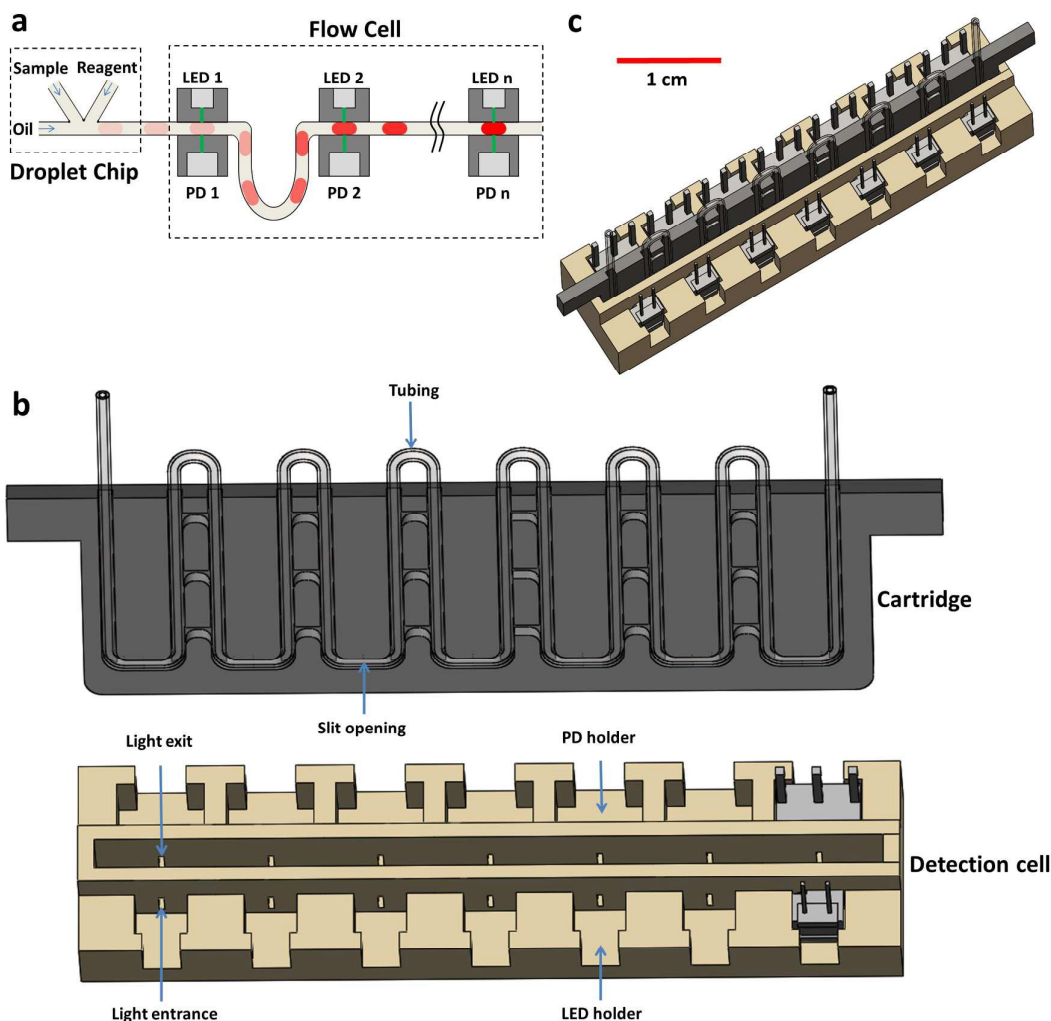
† Email: x.niu@soton.ac.uk

Fig. 1 Schematic of the multi-detector flow cell a) working principle of the device, b) 3D schematic of the flow cell showing the cartridge (top) which holds the tubing and the detection cell (bottom) which holds the LEDs and photodiodes. Both cartridge and detection cell have slits incorporated such that once the cartridge is inserted to the detection cell, there is a clear light path from LED to photodiode through the tubing, c) fully assembled flow cell.

to circumvent this is to measure the kinetics of the reaction – using the initial rate of colour development as the measure of analyte concentration. Several groups have recently reported this for static[21, 22] and oscillating[23] droplets using single-point detection, and for continuously flowing streams of droplets using multi-point detection[24-27].

The multi-point detection technique is perfect for the continuous measurement required for POC monitoring. Crucially, however, all of the previous reports employed sophisticated and bulky microscope-based setups unsuitable for application in clinical settings.

Here we present a miniaturised multi-detection point absorption flow-cell that allows high throughput continuous quantification analysis of metabolites and other biomarkers in droplet microfluidics. The small size (45 by 10 by 15 mm) and use of affordable components combined with its ability to perform continuous accurate biochemical quantification make

it highly suitable for use in field-deployable POC monitoring devices. In this paper we describe the design, and operation of the device and its validation by application to the accurate continuous quantification of unknown glucose concentrations using an enzymatic assay.

MATERIALS AND METHODS

Materials and reagents. Commercially available reagents were bought and used without further purification. Glucose oxidase, horseradish peroxidase, 4-aminoantipyrine, phenol and phosphate buffered saline (PBS) were purchased from Sigma Aldrich (Dorset, U.K). The reagents were prepared in 0.1 M PBS at pH of 7.4. The reagents were mixed such that the final reagent mixture consisted of glucose oxidase (30 U/mL), peroxidase (30 U/mL), 4-aminoantipyrine (1.54 mM) and phenol (22 mM). This solution of reagents will be referred as reagent mix in later sections. Glucose solutions were prepared

by dissolving glucose (Sigma Aldrich, U.K) in 0.1 M PBS at pH of 7.4. Ultrapure water was used throughout (18.2 MΩ·cm, MilliQ). Powdered red food dye (East End Foods plc) was used in solution for all calibrations.

Microchip fabrication. The T-junction chip used to generate droplets was fabricated as follows: Firstly, a mould was designed in 3D CAD software (SolidWorks, Dassault Systemes) and printed in VeroClear material using an Objet500 Connex3 3D printer (Stanford Marsh Ltd). The microchannels were designed to have dimensions of 200 µm in width and 400 µm in height. After printing, the surface of the mould was cleaned with isopropyl alcohol (IPA), dried and left in an oven overnight at 60 °C. The mould was further treated with a non-stick coating (Aquapel, PPG Industries) to aid removal of the polydimethylsiloxane (PDMS Sylgard 184) chip after casting. The PDMS channel layer was cast using the mould and bonded to another flat piece of PDMS using the standard 'half-cure' technique.[28]

Droplet generation. Droplets were generated using the T-junction microfluidic chip. The carrier fluid used was FC-40 fluorinated oil (3M, UK) containing a 0.35 % w/w concentration of non-ionic tri-block copolymer surfactant synthesised in-house.[29] Syringe pumps (PHD 2000/Harvard Apparatus) were used to pump all fluids, with the reagent mix and glucose solutions injected at the same flow rate and the flow rate of oil (1.31 µL/min) tuned to achieve droplets measuring approximately 10 nL. Following generation, the droplets flowed into a polytetrafluoroethylene (PTFE) tubing (0.4 mm ID, 0.7 mm OD, Adtech Polymer Engineering Ltd.) connected to the flow cell for optical detections.

Flow cell design and fabrication. The miniaturised multidetector flow cell was designed using SolidWorks as shown in Fig. 1 and printed in black poly(lactic acid) (PLA) material using an Ultimaker-2 3D printer. The flow cell is composed of two interlocking 3D-printed structures, cartridge and detection cell, as shown in Fig 1b. The cartridge holds the tubing in place and is inserted into the detector cell, which houses the main optical components.

The cartridge is 1 mm thick and has grooves cut into one side such that 0.7 mm OD PTFE tubing can snugly fit into it. The tubing can be inserted into the groove in numerous different geometries to give different distances (and hence travel time of the droplets) between detectors, as appropriate to the assay time being implemented. The cartridge has 7 horizontal slits (400 µm width) that allow light to pass through the tubing and the cartridge itself, and these horizontal slits are co-located with vertical slits (400 µm width) in the detection cell. The detection cell houses 7 pairs of light emitting diodes (LED, ASMT-QGBE-NFH0E, Avago Technologies) and photodetectors (PD, TSL257, Texas Advance Optical Solutions), each of which correspond to an individual absorption detection point. Here, green LEDs (peak wavelength = 516.5 nm) were used to coincide with the main absorption band of the colorimetric product of the glucose assay (peak value 545 nm). It should be noted, however, that the LEDs can be changed, depending on the exact colorimetric assay being implemented. Fig. 1c shows
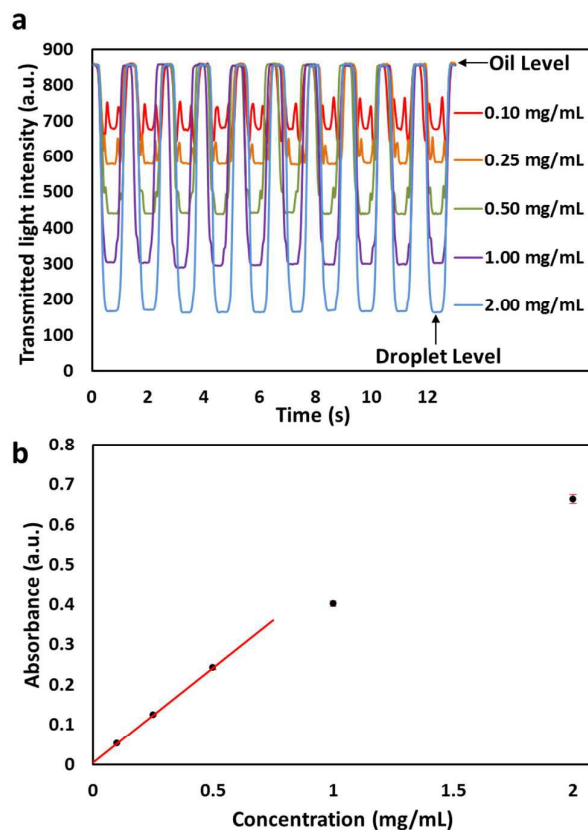

Fig. 2 Characterisation of a single detector in the flow cell using droplets containing red food dye. a) Transmitted light intensity over time as droplets travel through the light path. Five distinct populations of droplets with different dye concentrations are observed: 0.10, 0.25, 0.50, 1.00, 2.00 mg/mL. b) Droplet absorbance against dye concentration. A line of best fit (R^2 = 0.998) shows the linear response for absorbance values < 0.3.

the cartridge and detection cell in position for droplet detection.

Data processing. The voltage readout from each photodiode was collected using a microcontroller (Arduino Nano) which relayed the information in real-time to a computer, where the data was recorded using LabView (National Instruments).

Absorption values for the droplets were calculated using a modified version of the Beer-Lambert law (Eq. 1). To allow for small changes in the light intensity of the LED, the equation includes terms for the light transmitted through the carrier fluid. As the composition of the carrier fluid doesn't change, it will give a constant absorption and can thus be used to adjust for any changes in the intensity of incident light between the measurement of the blank and all subsequent measurements.

$$A = -log_{10}\left(\frac{I_{sample\ droplet}}{I_{blank\ droplet}} \times \frac{I_{blank\ oil}}{I_{droplet\ oil}}\right) = \varepsilon c l \qquad Eq.\ (1)$$

Where $I_{sample\ droplet}$ and $I_{blank\ droplet}$ are the photodiode responses corresponding to light transmitted through the sample droplets and blank droplets (introduced at the start of an experiment) respectively; $I_{blank\ oil}$ and $I_{droplet\ oil}$ are the

photodiode responses for light transmitted through the carrier fluid adjacent to the blank and sample droplets. Absorbance is equal to $\varepsilon c l$ where ε is the molar absorption coefficient, c the concentration and l the optical path length.

RESULTS AND DISCUSSION

The operation of the flow cell is illustrated in Fig 1a. Initially droplets composed of a 1:1 ratio of sample and reagent are generated with the T-junction microfluidic chip. Droplets exit the chip into PTFE tubing which is woven into the flow cell such that the droplets sequentially pass through each detector in turn. As the colorimetric reaction progresses, the colour of the droplet deepens and the absorbance as measured by each detector increases. The absorbance gives a measure of the concentration of the end-product from Eq.1. The time for a droplet to travel from the T-junction to the detection point was calculated by dividing the total length of channel and connection tubing with the flow speed. By measuring the absorbance of a droplet at all of the 7 detectors, the initial rate of reaction can be obtained.

Calibration of the flow cell

The flow cell was fabricated from off-the-shelf optical components and tubing inserted within 3D-printed structures, as shown in Fig 1b and c. Once fully assembled, the flow cell measures only 45 x 10 x 15 mm, therefore, it can be easily accommodated within a field-deployable POC device.

We initially characterised the single detectors within the flow cell by flowing droplets of red food dye at different concentrations through the flow cell and measuring the response.

Fig 2a shows the light intensity obtained for five series of droplets containing different dye concentrations (0.10, 0.25, 0.50, 1.00 and 2.00 mg/mL). As each droplet enters the light path the transmitted light intensity drops from a higher value (corresponding to light passing through the carrier oil) to a lower value. As the droplet exits the light path, the measured intensity returns to its initial high value. For the lowest concentrations, the entry and exit of the droplets is accompanied with a brief spike in the light intensity due to lensing by the droplet/oil interface. As the dye concentration increases, this effect becomes less noticeable as it becomes masked by the higher absorbance of the droplet.

The detector shows a high reproducibility for each group of droplets, with percent relative standard deviations (%RSD) of the light transmitted through the droplets below 0.5 %. As the dye concentration in the droplets drops from high to low, the magnitude of the intensity drop also decreases – consistent with the absorbance of less light, as we would expect. The absorbance of each concentration of droplets was calculated against a set of blank droplets composed of pure water using the modified Beer-Lambert law (see Methods). Each concentration was repeated 3 times and the overall %RSD was found to be ~ 2 %. Fig 2b shows the measured absorbance values *versus* dye concentration.

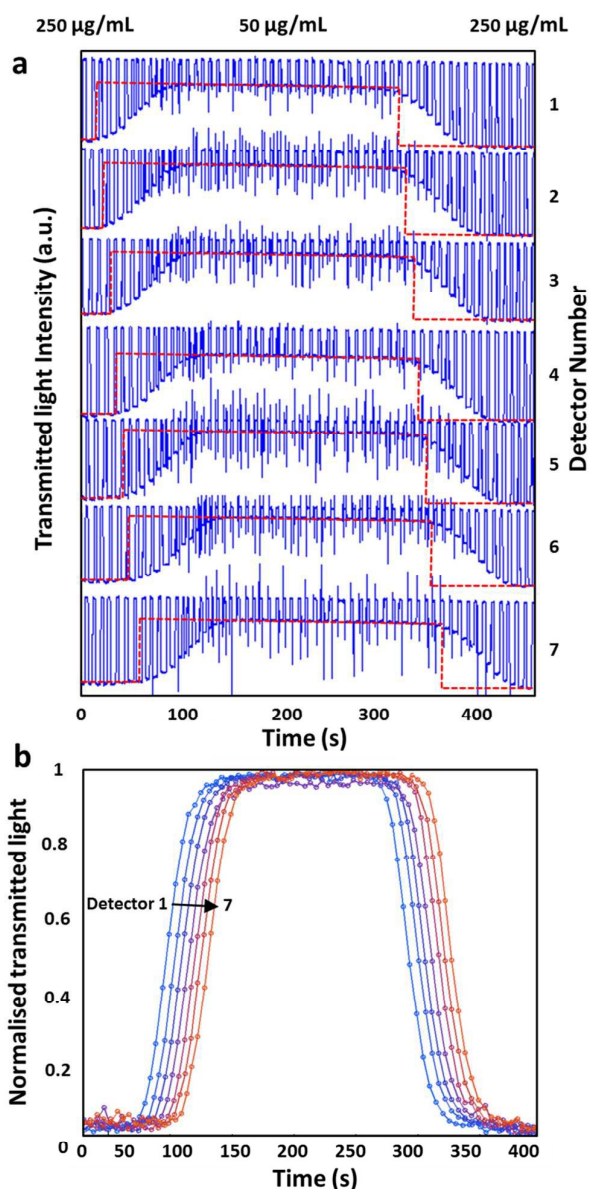As expected a linear relationship is seen at lower concentrations with deviation from linearity at

Fig. 3 Characterisation of the multi-detector flow cell using red food dye. a) Absorbance from 7 detectors (top to bottom) with changing dye concentration from high (250 μg/mL) to low (50 μg/mL) and to high again. The red dotted lines indicate where the concentration was switched and along the detectors. b) Normalised transmitted light plot against time illustrates that the profile of concentration switch is identical at each detector. Each point in the figure represents a single droplet.

absorbances > 0.25.[30] The limit of detection, defined as three times the standard deviation of a series of blank measurements, was found to correspond to an absorbance of 0.01. This value could be further improved by increasing the optical path length by, for example, controlling the channel geometry [14] or implementing cavity mirror enhancement.[15] These measurements confirmed that the absorption flow cell can be used to perform quantitative
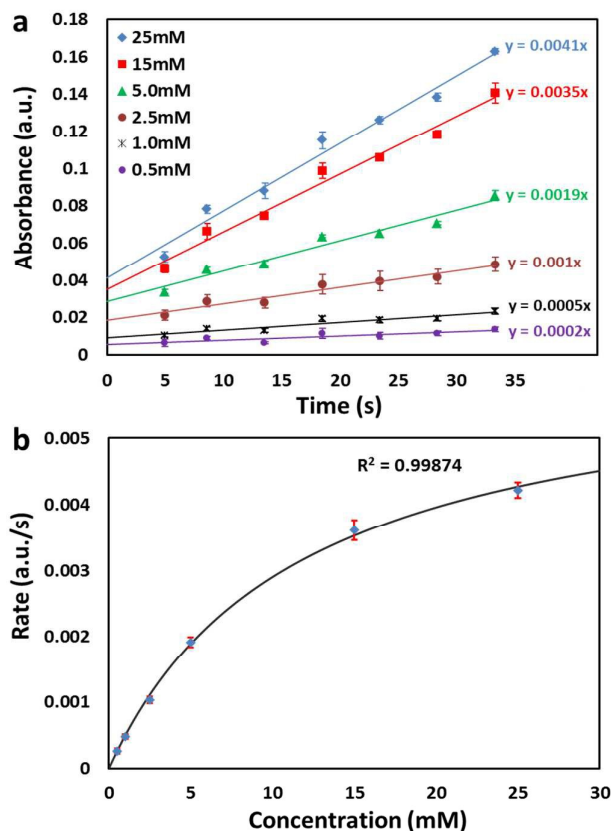
Fig. 4 Use of the flow cell in determining glucose concentrations with a Trinder's assay. a) Absorbance of droplets flowing through the flow cell, expressed in relation to the time since generation. Each result is a repeat of three separate experiments with the standard deviation expressed as the error bars (mean 6.4 % RSD). The lines of best fit constitute the initial reaction rate and are shown plotted against the glucose concentration in b). The data is fitted by nonlinear regression with a Michaelis-Menten curve.
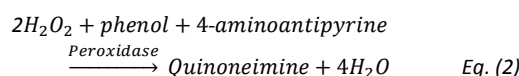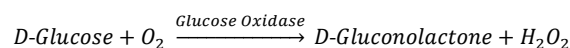
absorption measurement and has an operational range between absorbance values of 0.01 and 0.25.

Next the dye solution entering the droplet generation chip was alternatively swapped between a high concentration (250 µg/mL) and a low concentration (50 µg/mL). Figure 3a shows the measured signals from all 7 detectors. For each detector, the carrier oil gave constant high signals, while the response of the droplets changed with the concentration change. In the experiment, about 14 droplets and a time of 25s were required to switch from one concentration to the other completely. The red dotted lines in Fig 3a highlight the onset of the transitions. Comparing the signals from these 7 detectors, it can be seen that the onset of transition times shift sequentially to the right (later time) following the sequential order of the detectors. This trend is more apparent in Fig 3b, which shows the same data normalised such that each point represents the measured average light intensity of a single droplet. This plot also emphasises that the shape of the transitions is identical for each detector and the train of droplets travels between detectors without the cross contamination or Taylor dispersion commonly found in continuous microfluidic sensors [31]. Additionally it also shows the high-throughput nature of the flow cell, as individual droplets can be identified in each subsequent flow cell

detector, thus each droplet constitutes a single discrete set of measurements.

Glucose enzymatic assay

Having calibrated the flow cell using food dye, a colorimetric assay was implemented to quantify glucose concentrations in sample solutions. Glucose measurement was chosen because it is a widely measured biomarker for a range of medical conditions and procedures including metabolic diseases [3], diabetes [4], traumatic brain injury [6] and free flap surgery.[7] Glucose can be determined *via* an enzyme-based colorimetric assay based on Trinder's reaction [32] as shown in Eq. 2.

$$D\text{-}Glucose + O_2 \xrightarrow{\text{Glucose Oxidase}} D\text{-}Gluconolactone + H_2O_2$$

$$2H_2O_2 + phenol + 4\text{-}aminoantipyrine$$
$$\xrightarrow{\text{Peroxidase}} Quinoneimine + 4H_2O \qquad Eq.\ (2)$$

Glucose oxidase oxidises glucose in the presence of oxygen to form gluconolactone and hydrogen peroxide. The hydrogen peroxide reacts with 4-aminoantipyrine in the presence of horseradish peroxidase to yield violet-coloured quinoneimine which absorbs light at a maximum of 545 nm.

Lee et al. [33] have previously used this method to measure glucose after the reaction has gone to completion. However, the reaction can take up to 30 min [Cayman glucose colorimetric assay kit, Item no 10009582] - too long for acute care patients where real-time or near real-time (tens of seconds delay) monitoring would be highly beneficial.[3] Another method is to measure the initial reaction rate, and accurate measurements of analyte concentrations can be obtained within 1 minute. [34]

In order to convert the measured reaction rates to a known concentration, the method must first be calibrated using the Michaelis-Menten model [35-36] which relates the initial rate of reaction (V_0) to the concentration of the substrate (glucose in this case) as shown in Eq. 3.

$$V_0 = \frac{V_{max} \cdot [S]}{[S] + K_m} \qquad Eq.\ (3)$$

Where [S], V_{max} and K_m are the substrate concentration, maximum rate at saturating substrate concentration, and substrate concentration at half the maximum rate ([S] at ½V_{max}). V_{max} and K_m are constants at constant temperature and constant enzyme concentrations, therefore, V_0 increases with substrate concentration [19].

For the calibration, droplets composed of a glucose solution and reagent (containing glucose oxidase, peroxidase, phenol and 4-aminoantipyrine) mixed at a 1:1 ratio were generated and then flowed through the flow cell. This was repeated using six different known glucose concentrations (0.5, 1.0, 2.5, 5.0, 15 and 25 mM). Blank measurements were taken by using 0 concentration glucose solution and used to calculate the absorbance of the glucose-containing droplets. In the experiment, the droplet flow rate was kept constant and we measured droplets passed through detectors (1-7) at times of 4.94, 8.58, 13.52, 18.46, 23.4, 28.34 and 33.28 seconds
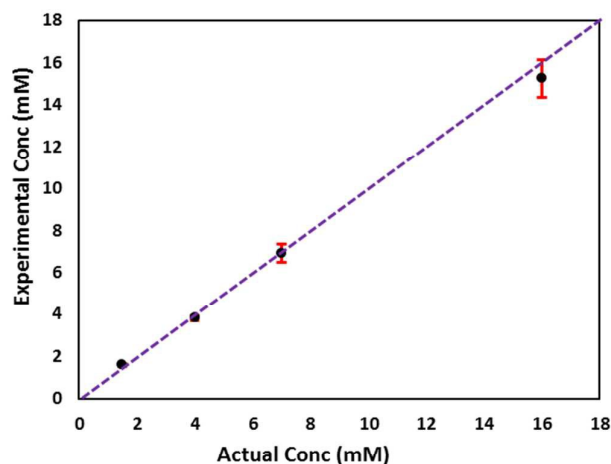
Fig. 5 Comparison of the experimentally-determined concentrations of a series of glucose solutions versus their actual concentrations. The experiments were carried out in triplicate and the standard deviations are expressed as the error bars. The dotted line shows the 1:1 equivalence.

respectively (the time was defined to be 0 at the moment when the droplet was generated at the T-junction.)

Fig 4a shows the absorbance against time for each set of glucose concentrations. For each glucose concentration, the absorbance increased linearly as expected and was fitted with a straight line to obtain the initial reaction rate. It is notable that none of the lines of best fit pass through the origin, indicating that the reaction had started before t = 0. This is likely to be due to the reaction having started in the T-junction at the interface where the two aqueous streams met, before they had been partitioned into droplets. Nonetheless, the shift of origin time does not affect the measurement of reaction rate which is the slope of the line. The obtained reaction rates were then plotted against the glucose concentration and fitted with a Michaelis-Menten curve using nonlinear regression, (see Fig 4b). The curve fits the data exceptionally well ($R^2 \approx$ 0.999) with V_{max}= 0.0062 a.u./s and K_m= 11.52 mM.

Having obtained the Michaelis-Menten curve and along with it, the values for V_{max} and K_m, it was then possible to use the flow cell to determine the glucose content of unknown solutions. To confirm this and to test the accuracy of the flow cell, we formulated four new glucose solutions (1.5, 4, 7 and 16 mM) as 'unknown' samples and determined their concentrations from their initial reaction rates. Droplets of these 'unknown' samples were generated and taken through the flow cell as before. The linear increases in absorbance of the droplets with time were recorded and the initial reaction rates obtained from the gradient of the lines of best fit. The concentrations of glucose were calculated by using a rearranged form of the Michaelis-Menten equation:

$$[S] = \frac{V_0 . K_m}{V_{max} - V_0} \qquad Eq. (4)$$

The experiments were carried out in triplicate and the recovered concentrations were 1.59, 3.80, 6.90 and 15.3 mM, with small average errors of <5% RSD. These measured concentrations are plotted against the actual concentrations in

Fig. 5. It is interesting to note that the error (as shown by the error bars) increases with concentration, which is likely due to the increased influence of experimental error in Eq. 4. V_0 increases with concentration and as it becomes more significant with respect to V_{max}, so too does the error contained within the denominator of Eq. 4. Nonetheless, the relative error is still small and the measured concentrations are in excellent agreement with the actual values. This shows that, despite being small in size and being fabricated from low-cost components, the flow cell can be used for accurate quantitative analysis metabolite concentration *via* measurement of enzymatic kinetics.

In addition to the high accuracy just demonstrated, the flow cell is intrinsically high throughput making it suitable for POC monitoring by continuous measurement of a time sequence of sample droplets. To demonstrate this, the glucose concentration in the droplets was changed sequentially using a similar method to Fig. 3, with stabilised concentrations at 4, 6.5 and 16 mM. Droplets were automatically identified from the detected signals using computer code written in Matlab (Mathworks). The absorbance of each droplet at different detectors was correlated with reaction time and the initial reaction rates were obtained from lines of best fit. This gave the reaction rate for each droplet, as shown in Fig. 6a. These reaction rates were then converted to give the glucose concentration for each sample droplet using Eq. 4. as shown in Fig. 6b. Each point constitutes a distinct measurement with a time interval of 4.2 s between neighbouring droplets in this experiment. While this frequency should be more than
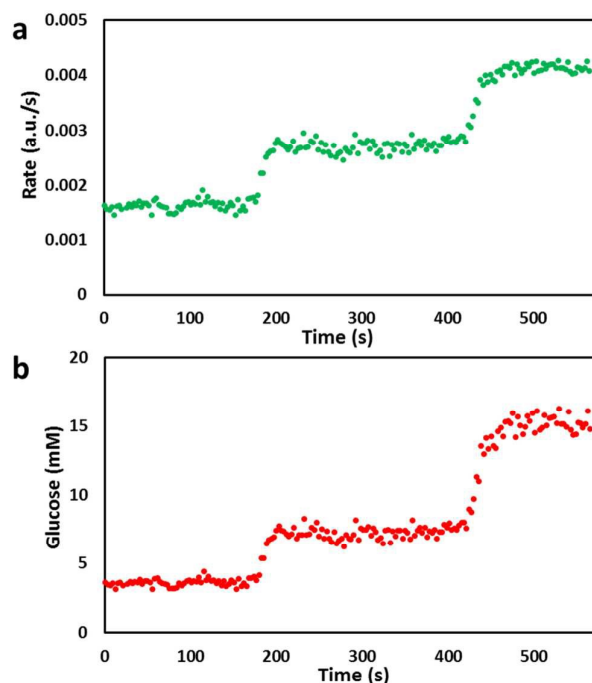

Fig. 6 High throughput determination of glucose concentration in the flow cell. a) Initial rate of reaction of droplets flowing through the flow cell, expressed in relation to the time since generation, b) Actual concentration of each droplet calculated via rearranged Michaelis-Menten equation.

ARTICLE

sufficient for most POC applications (e.g. glucose monitoring), even higher measurement frequencies could be obtained by simply increasing the linear velocity of the droplets while also extending the length of tubing in between detectors to provide enough reaction time.

CONCLUSIONS

We have developed a multidetector flow cell for the study of enzymatic reactions within microdroplets. The flow cell has been successfully applied to glucose analysis and determination of unknown samples using Michaelis-Menten kinetics. This 'mix-and-read' glucose assay represents a large class of homogeneous and heterogeneous enzymatic assays routinely performed in biomedical labs, therefore, the device may find wide applications in the measurement of other biomolecules for example, lactate, pyruvate, etc. The flow cell has a small footprint made of low-cost components, makes it a suitable choice to be integrated in portable or even wearable point-of-care applications. There are recent exciting developments on 'digitalising' various continuous chemical signals into sequential droplets.[37-38] Our device can measure these sequential droplets colorimetrically and without stopping flow, enabling continuous and near real-time monitoring with droplet microfluidics.

ACKNOWLEDGEMENTS

REFERENCES

1   A. S. John and C. P Price, *The Clinical Biochemist Reviews*. 2014, 353, 155-167.
2   C. D. Chin, V. Linder and S. K. Sia, *Lab Chip*, 2012, 12, 2118–2134
3   M. L. Rogers, M. G. Boutelle, *Annu. Rev. Anal. Chem*, 2013, 6, 427–53.
4   M. Montagnana, *et al., Clinica Chimica Acta*, 2009, 402, 7–13.
5   S. Vaddiraju, D, J. Burgess, I. Tomazos, F. C. Jain, F. Papadimitrakopoulos, *J Diabetes Sci Technol*, 2010, 4, 1540-1562.
6   P. Hashemi, R. Bhatia, H. Nakamura, J. P. Dreier, R. Graf, A. J. Strong, M. G. Boutelle, *J Cereb Blood Flow Metab*, 2009, 29, 166-175.
7   M. Rogers, P. Brennan, C. Leong, S. Gowers, T. Aldridge, *et al., Anal. Bioanal. Chem*, 2013, 405, 3881–88.
8   S. A. Gowers, V. F. Curto, C. A. Seneci, C. Wang, S. Anastasova, P. Vadgama, G. Z. Yang, M. G. Boutelle, *Anal. Chem*, 2015, 87, 7763–7770.
9   H. Haugaa, E. B. Thorgersen, A. Pharo, K. M. Boberg, A. Foss, P. D. Line, T. Sanengen, R. Almaas, G. Grindheim, S. E. Pischke, T. E. Mollnes, T. Tonnessen, *Liver Transpl,* 2012, 18, 839-49.
10   A. Galvan, Y. Smith, T. Wichmann, J Neurosci Methods, 2003, 126, 175-85.
11   W. Gao, S. Emaminejad, H. Y. Y. Nyein, S. Challa, K. Chen, A. Peck, H. M. Fahad, H. Ota, H. Shiraki, D. Kiriya, D. Lien, G. A. Brooks, R. W. Davis, and A. Javey, *Nature*, 2016, 529, 509–514.
12   J. Wang, *Chem. Rev. 2008, 108, 814–825*.
13   A. K. Ellerbee, S. T. Phillips, A. C. Siegel, K. A. Mirica, A. W. Martinez, P. Striehl, N. Jain, M. Prentiss and G. M. Whitesides, *Anal. Chem,* 2009, 81, 8447–8452.
14   J. V. Sieben, C. F. A. Floquet, I. R. G. Ogilvie, M. C. Mowlem and H. Morgan, *Anal. Methods*, 2010, 2, 484.
15   C. M. Rushworth, G. Jones, M. Fischlechner, E. Walton and H. Morgan, *Lab Chip*, 2015, 15, 711.
16   C. A. Burtis, R. A. Edward, and D. E. Bruns. *Tietz textbook of clinical chemistry and molecular diagnostics*. Elsevier Health Sciences, 2012.
17   H. Song, J. D Tice, R. F. Ismagilov, *Angew Chem Int Ed Engl,* 2003, 42, 768-772.
18   D. R. Link, , E. Grasland-Mongrain, A. Duri, , F. Sarrazin, Z. D. Cheng, G. Cristobal, M. Marquez, D. A. Weitz, *Angew. Chem., Int. Ed,* 2006, 45, 2556–2560.
19   D. L Nelson, M. M. Cox, Lehninger Principles of biochemistry, W.H. Freeman. 2008.
20   S. Mamoru, H. Kazuyuki, *Clin Chim Acta.,* 1977, 75, 387-91.
21   Srinivasan, V., et al., *Analytica Chimica Acta*, 2004, 507, 145–150.
22   E. Fradet, C. Bayer, F. Hollfelder and C. N. Baroud, *Anal. Chem,* 2015, 87, 11915–11922.
23   F. Gielen, L. V. Vliet, B. T. Koprowski, S. R. A. Devenish, M. Fischlechner, J. B. Edel, X. Niu, A. J. deMello, and F. Hollfelder, *Anal. Chem,* 2013, 85, 4761–4769.
24   N. Damean, L. F. Olguin, F. Hollfelder, C. Abella and W. T. S. Huck, *Lab Chip*, 2009, 9, 1707–1713.
25   S. Jambovane, D. J. Kim, E. C. Duin, S. Kim, and J. W. Hong, *Anal. Chem*, 2011, 83, 3358–3364.
26   D. Hess, A. Rane, A. J. deMello and S. Stavrakis, *Anal. Chem*, 2015, 87, 4965–4972.
27   S. L. Sjostrom, H. N. Joensson and H. A. Svahn, *Lab Chip*, 2013, 13, 1754–1761.
28   M. A. Unger, H. Chou, T. Thorsen, A. Scherer, S. R Quake, *Science*, 2000, 288, 113.
29   V. Chokkalingam, Tel J, F. Wimmers, X. Liu, S. Semenov, J. Thiele, C. G. Figdor, W. T. Huck, *Lab Chip*, 2013, 13, 4740-4.
30   A. D. Beaton, C. L. Cardwell, R. S. Thomas, V. J. Sieben, F. Legiret, E. M. Waugh, P. J. Statham, M. C. Mowlem, H. Morgan, 2012, *Lab Chip*, 2012, 46, 9548-9556.
31   I. R. G. Ogilvie, V. J. Sieben, M. C. Mowlem and H. Morgan, *Anal. Chem*, 2011, 83, 4814–4821.
32   P. Trinder, *Ann. Clin. Biochem*, 1969, 6, 24.
33   Y. Lee, S. Shin, T. Shigihara, E. Hahm, M.Liu, J.Han, J. Yoon and H. Jun, *DIABETES*, 2007, 56, 1671-1679.
34   P. Abrahamsson, O. Winso, *Journal of Pharmaceutical and Biomedical Analysis*, 2005, 730–734.
35   T. Laurell, J. Drott, *Biosens. Bioelectron,* 1995, 10, 289.
36   J. Wang, *Electrophoresis,* 2002, 23, 713.
37   X. Niu, B. Zhang, R. T. Marszalek, O. Ces, J.B. Edel, D. R. Klug, and A. J. deMello, 2009, *Chem Comm*, 41, 6159-6161.
38   M. Wang, G. T. Roman, K. Schultz, C. Jennings and R. T. Kennedy, *Anal. Chem*, 2008, 80, 5607–5615.

Analyst Accepted Manuscript